**Article:**
Olumayegun, O. and Wang, M. (2019) Dynamic modelling and control of supercritical CO2 power cycle using waste heat from industrial processes. Fuel, 249. pp. 89-102. ISSN: 0016-2361

https://doi.org/10.1016/j.fuel.2019.03.078

# Dynamic Modelling and Control of Supercritical $CO_2$ Power Cycle Using Waste Heat from Industrial Processes

**Olumide Olumayegun, Meihong Wang***

Department of Chemical and Biological Engineering, University of Sheffield, Mappin Street, Sheffield, S1 3JD, United Kingdom

*Corresponding author.

E-mail addresses: o.olumayegun@sheffield.ac.uk (O. Olumayegun), Meihong.Wang@sheffield.ac.uk (M. Wang)

## Abstract

Large amount of waste heat is available for recovery in industrial processes worldwide. However, significant proportion (up to 50%) of this thermal energy is released directly to the environment. Application of waste heat to power (WHP) technologies can increase the energy efficiency and cut $CO_2$ emissions from these facilities. Steam Rankine cycle (SRC) and organic Rankine cycle (ORC) are commonly deployed for this purpose. The main drawback of SRC and ORC is the high irreversibility in the heat exchangers. In addition, ORC has limited temperature range and low efficiency while SRC has a large footprint. Supercritical $CO_2$ ($sCO_2$) power cycle is considered an attractive option, which provides better matching of waste heat temperature in the main heater (i.e. low irreversibility). It offers compact design, improved performance and it is applicable to a wide range of waste heat source temperature. The conditions of industrial waste heat sources are highly variable due to continuous fluctuations in the operation of the process. This is likely to significantly affect the dynamic performance and operation of the $sCO_2$ power cycle. In this work, dynamic model in Matlab/Simulink was developed to assess the dynamic performance and control of the $sCO_2$ power cycle for waste heat recovery from cement industry. The case of waste heat at 380 $^0$C utilized to deliver 5 MWe of power was considered. Steady state simulation was performed to determine the design point values. Open loop simulation was performed to show the inherent dynamic response to step change in the temperature of the waste heat. The dynamic performance and control of the system under varying exhaust gas flow rate between 100% and 50% of the design value were studied. Similar study was done for varying exhaust gas temperature between 380 $^0$C and 300 $^0$C. The results showed that the thermal efficiency of proposed single recuperator recompression $sCO_2$ is about 33%. Stable operation of the system can achieved by using cooling water control and throttle valve to maintain constant precooler outlet condition. Dynamic simulation result showed that it is best to allow the turbine inlet temperature to vary according to the fluctuation in the waste heat source. These findings indicated that dynamic modelling and simulation of WHP system could contribute to understanding of the behaviour and control system development under fluctuating waste heat source conditions.

# Graphical abstract

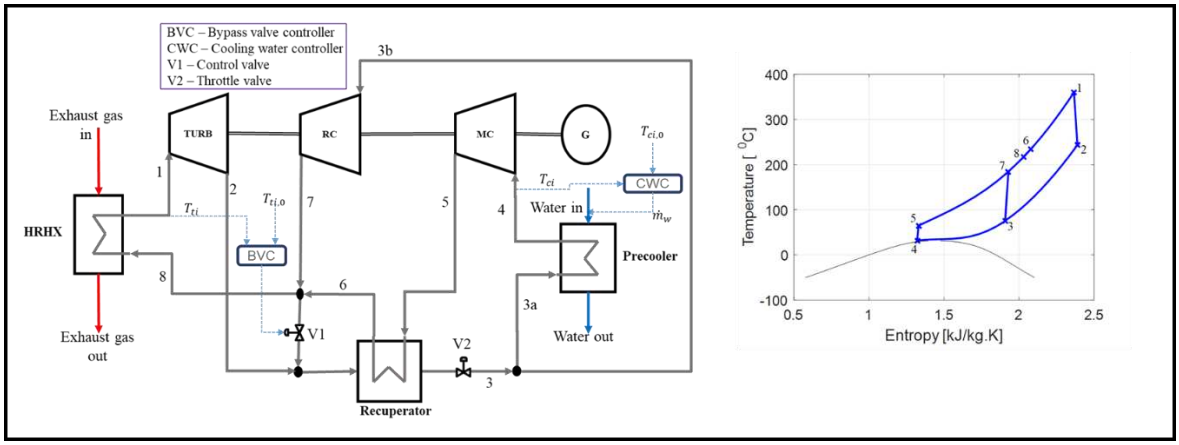



# Keywords

Waste heat recovery

Cement industry

Supercritical $CO_2$ cycle

Dynamic modelling

PID control

Industrial processes


# Highlights

- Dynamic model development in Matlab/Simulink proposed
- Analysis of control strategy for the WHR system
- Dynamic performance evaluation under varying heat source condition
- Supercritical $CO_2$ power cycle is promising for WHR application

# Nomenclature and Units

## Abbreviations

| | |
|---|---|
| BVC | Bypass valve controller |
| CWC | Cooling water controller |
| G | Generator |
| HRHX | heat recovery heat exchanger |
| MC | main compressor |
| NIST | National Institute of Standards and Technology |
| ORC | organic Rankine cycle |
| PCHE | Printed Circuit Heat Exchanger |
| PID | Proportional-Integral-Derivative |
| RC | Recompression compressor |
| $sCO_2$ | supercritical carbon dioxide |
| SRC | steam Rankine cycle |
| T-S | temperature-entropy |

| | |
|---|---|
| $tCO_2$ | transcritical carbon dioxide |
| TURB | turbine |
| WHP | waste heat to power |
| WHR | waste heat recovery |

60

61 # Symbols

| | |
|---|---|
| $C$ | Specific heat capacity (J/kg.K) |
| $C_v$ | Constant valve construction coefficient ($m^2$) |
| $e(t)$ | Error signal |
| $h$ | Specific enthalpy (kJ/kg) |
| $J$ | Inertia ($kg.m^2$) |
| $K_d$ | Derivative gain of PID controller |
| $K_i$ | Integral gain of PID controller |
| $K_p$ | Proportional gain of PID controller |
| M | Mass (kg) |
| $\dot{m}$ | Mass flow rate (kg/s) |
| $P$ | Pressure (Pa or $N/m^2$) or Power (W or J/s) |
| $PR$ | Pressure ratio |
| $Q$ | Heat duty (watt or J/s) |
| $T$ | Temperature (K) |
| $t$ | time (second) |
| $U$ | Impeller tip speed (rad/sec) |
| $u(t)$ | Control signal |
| $V$ | Volume ($m^3$) |
| $y$ | Fraction valve opening |
| $\gamma$ | Relative pressure loss or friction loss coefficient ($m^{-4}$) |
| $\eta$ | Efficiency |
| $\kappa$ | Constant of proportionality for heat transfer coefficient |
| $\tau$ | Time constant (seconds) |
| $\rho$ | Density ($kg/m^3$) |
| $\phi$ | Flow coefficient |
| $\psi$ | Pressure ratio coefficient |
| $N$ | Rotational speed (rev/s) |

62

63 # Subscripts

| | |
|---|---|
| 0 | Set point |
| $c$ | Compressor or cold stream |
| $gen$ | Generator |
| $h$ | Hot stream |
| $in$ | inlet |
| $isen$ | Isentropic |
| $load$ | Electrical load |
| $mc$ | Main compressor |
| $out$ | Outlet |
| rc | Recompression compressor |
| $t$ | Turbine |
| $w$ | Metal wall |

64

# 1 Introduction

Increased concentration of anthropogenic $CO_2$ in the atmosphere due to fossil fuel combustion is widely believed to be responsible for global warming and extreme climate change. In particular, industrial processes are energy intensive, up to 70% of the energy is provided by fossil fuel and about 40% of global $CO_2$ emissions are attributable to the industrial sector [1]. Hence, reduction of $CO_2$ emissions from industrial processes is critical to achieving the target of keeping global temperature rise to well below $2^0$C above pre-industrial levels as set out in the Paris Agreement at COP 21 in 2015. In a typical cement industry, it is estimated that about 40% of the input fuel energy is lost in the waste heat streams [2, 3]. Therefore, the use of waste heat to power technologies (WHP) to recover some of the thermal energy can increase the energy efficiency and reduce $CO_2$ emissions from these facilities.

Organic Rankine cycle (ORC) and steam Rankine cycle (SRC) are commonly investigated for waste heat recovery (WHR) applications [4-11]. However, ORCs are mostly restricted to low heat source temperatures below 300 $^0$C due to risk of decomposition of the organic fluid [10, 12] while SRCs tend to have large plant footprint. On the other hand, supercritical and trans-critical $CO_2$ power cycles have been identified in several studies as a promising technology for both low, medium and high temperature WHR. In supercritical cycle (Figure 1a), the working fluid operates entirely above its critical pressure while in trans-critical cycle (Figure 1b), the working fluid passes through both subcritical conditions and supercritical conditions [13]. The main benefits of $CO_2$ based power cycles compared to ORC and SRC include [14-17]: (a) it is applicable to a wide range of temperature (up to 1000 $^0$C); (b) less irreversibility in the recovery heat exchanger i.e. better temperature profile matching between the waste heat and the working fluid; (c) improved performance even at temperature below 400 $^0$C; (d) it is non-toxic, non-flammable and non-corrosive; (e) it has low global warming potential (GWP); and (6) it is more compact compared to SRC.

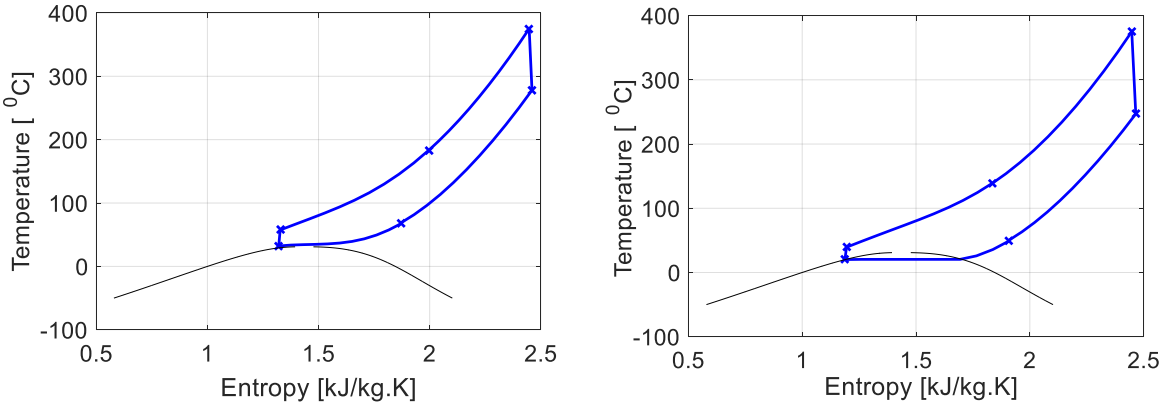


(a) Supercritical $CO_2$ cycle (b) Trans-critical $CO_2$ cycle

Figure 1: Temperature-Entropy diagrams of supercritical and trans-critical $CO_2$ power cycles

Karellas et al. [18] performed energetic and exergetic analysis of SRC and ORC WHR systems in the cement industry and concluded that WHR can significantly reduce electricity consumption operating cost. Chen et al [19] compared the performance of trans-critical $CO_2$ (tCO2) cycle with an ORC using R123 as working fluid for WHR applications. The study showed that the $CO_2$ power cycle has a higher efficiency than the ORC due to better temperature matching between the waste heat source and the $CO_2$ working fluid. There is no pinch limitation in the recovery heat exchanger of the $CO_2$ cycle. Sarkar [16] presented a comprehensive review of supercritical $CO_2$ ($sCO_2$) power cycle for waste heat conversion and highlighted its benefits and future trends. Detailed analysis based on energy, exergy, finite size thermodynamics and heat exchanger's surface for a $CO_2$ transcritical power cycle using industrial low-grade heat source was presented by Cayer et al [20]. The calculations were carried out for fixed temperature and mass flow rate of the heat source, fixed turbine inlet and cooler outlet temperature in the cycle and fixed sink temperature to determine the optimum maximum cycle pressure. Wang and Dai [21] performed exergetic and economic analysis for a cascaded $sCO_2$/$tCO_2$ cycle for waste heat

recovery and compared the performance to a $sCO_2$/ORC system. The results showed that the $sCO_2/tCO_2$ system performs better than the $sCO_2$/ORC system.

Various layouts have been investigated in the literature for improving the performance of supercritical/trans-critical $CO_2$ power cycle. Mondal and De [22] investigated the implementation of multi-stage compression and intercooling for possible improvement of the performance of $CO_2$ based power cycle using low temperature waste heat. The developed thermodynamic model indicated the existence of an optimum combination of the cycle minimum pressure and the intermediate pressure. For engine WHR, Shu et al [23] suggested an improved $CO_2$ based power cycle containing a preheater and a recuperator. The improved $CO_2$ based power cycle gives better performance compared to the basic cycle and the ORC. Thermodynamic modelling of a recompression $CO_2$ power cycle for WHR was performed by Banik et al [24] for potential higher cycle efficiency. The thermodynamic performance of basic recuperated $sCO_2$ cycle is limited by heat capacity mismatch in the recuperator. The recompression $sCO_2$ cycle, which has two recuperators, is commonly used to minimise the effect of heat capacity mismatch in the recuperator. Olumayegun [25] suggested the single recuperator recompression cycle for low temperature heat source. The single recuperator recompression $sCO_2$ cycle also resolves the heat capacity mismatch and it is simpler than the recompression cycle layout. This cycle is proposed in this study for WHR application.

Li et al. [26] reported the results of preliminary tests on dynamic characteristics of $tCO_2$ power cycle in a kW-scale test bench for recovering exhaust energy from a diesel engine. Experimental data for dynamic responses to changes in $CO_2$ pump speed and expansion valve pressure ratio were presented. However, test bench facilities are usually too small to include all the major components and attributes of a commercial scale plant. Hence, Alobaid et al. [27] emphasized the application of dynamic modelling and simulation as an inexpensive tool for the analysis of power plant under different transient operating conditions and for control system development in their comprehensive review of dynamic modelling of various thermal power plant. Compared to $sCO_2/tCO_2$ based power cycle, the dynamic modelling and simulation of ORC/SRC for WHR have received much more attention [28 - 32]. Jiménez-Arreola et al [31] studied the dynamics of ORC evaporator under fluctuating waste heat source condition with particular focus on the influence of the evaporator geometry and materials. Quoilin et al. [29] employed dynamic modelling to predict the dynamic behaviour and compared three different control strategies under varying flow rate and temperature of waste heat source for a small-scale ORC. Sun et al [32] investigated dynamic optimal design of SRC utilising industrial waste heat with fluctuating temperature and mass flow rate of exhaust gas.

In the literature, only few modelling and simulation studies have been conducted to understand the dynamic behaviour and control of $sCO_2$ based power cycle for waste heat applications. Most modelling studies on the development of $sCO_2$ power cycle for WHR concentrate on the steady state performance evaluation through energetic and exergetic analysis, optimisation of design parameters, system configurations and economic analysis under a constant heat source condition. However, the mass flow rate and temperature of industrial waste heat sources are highly variable due to continuous fluctuations in the operation of the industrial processes [33]. This will significantly affect the dynamic performance and operation of the $sCO_2$ power cycle. Li et al [34] presented the results of dynamic modelling of trans-critical $CO_2$ power cycle for WHR in gasoline engines considering the system sensitivity to the external inputs. However, the study did not investigate the design of the control systems. Park et al. [35] performed dynamic model validation of $sCO_2$ experiment loop and simulation of transient responses to varying conditions such as valve control to simulate cycle operation, power swing to simulate load following and heat sink reduction to simulate failure. Osoro et al. [36] studied the dynamic behaviour under different seasonal conditions of concentrated solar power sCO2 cycle for system optimisation. The optimisation produced an increase in operating time from 220 to 480 minutes. Milani et al. [37] presented the results of dynamic modelling and control strategies for optimising the operating conditions of solar- and fossil-based $sCO_2$ recompression Brayton cycle. The model was used to investigate the performance of the plant with maximisation of solar input, minimisation of fossil fuel back up, direct solar heat input and indirect solar heat input.

To the authors' knowledge, dynamic modelling and control of single recuperator recompression $sCO_2$ cycle for WHR has not been reported so far. A dynamic model is required to investigate system transients and to test control strategies during changes in the mass flow rate and temperature of the waste heat source. In this study, dynamic model in Matlab/Simulink is developed to simulate and assess the transient characteristics and for control systems design of a single recuperator recompression $sCO_2$ power cycle for industrial WHR. Steady state simulation and preliminary design of heat exchangers are performed to obtain the design point values and input parameters for the dynamic model. Open loop simulation is performed to understand the inherent transient response to changes in the mass flow rate and temperature of the waste heat source. The dynamic performance and control of the system under varying mass flow rate and temperature of waste heat are simulated and analysed. In summary, the original contributions of this paper include: (1) application of single recuperator recompression $sCO_2$ cycle for WHR and the preliminary sizing on the heat exchangers; (2) dynamic modelling of a single recuperator recompression $sCO_2$ cycle for WHR application; and (3) design of PID-based control systems for variable waste heat sources.

The paper is organised as follows: Section 2 describes the configuration of the proposed $sCO_2$ power cycle for WHR application; Section 3 presents the derivation of the dynamic models of the system components and their integration in Simulink environment; Section 4 explains the control strategy to be implemented for the system; Section 5 discusses the results of the dynamic simulation of the system. Conclusions are given in Section 6.

# 2 System configuration and description

As already mentioned, the selected cycle configuration is the single recuperator recompression $sCO_2$ closed Brayton cycle layout. The system is designed to recover waste heat in the flue gas coming from an upstream industrial process and to covert the recovered waste heat to electrical power. The schematic layout of a single recuperator recompression $sCO_2$ closed Brayton cycle is presented in Figure 2 and the corresponding temperature-entropy (T-S) diagram is shown in Figure 3. The cycle consists of six main components: (1) a heat recovery heat exchanger (HRHX); (2) a recuperator; (3) a precooler; (4) a turbine (TURB) (5) the main compressor (MC); and (6) a recompression compressor (RC). The waste heat in the flue gas from the industrial process is recovered in the HRHX to heat the $CO_2$ working fluid to the turbine inlet temperature (point 1). The hot working fluid expands in the turbine (process 1-2) and converts the thermal energy of the working fluid to mechanical power. In the recuperator, the turbine exhaust enters the hot side (process 2-3) and is used to preheats the $CO_2$ exiting the MC. The working fluid leaving the hot side of the recuperator is split into two streams. One stream (3a) enters the water-cooled precooler (process 3a - 4) where heat is rejected to the environment and the working fluid is cooled down to the MC inlet temperature (point 4). The temperature and pressure of $CO_2$ at the MC inlet is above the critical point conditions such that the cycle is fully supercritical. The second stream (3b) is sent to the RC inlet. Both MC (process 4 – 5) and RC (process 3b - 7) increase the working fluid pressure. After the MC, the high-pressure working fluid is preheated by the turbine exhaust in the recuperator (process 5 – 6). The flow split fraction of stream 3 can be selected so that the heat capacity of $CO_2$ on the cold side of the recuperator match the heat capacity of $CO_2$ flowing through the hot side. An optimal selection of the flow split fraction will result in high recuperator effectiveness and improved thermal efficiency of the cycle. The preheated working fluid leaving the cold side of the recuperator is mixed with the high-pressure working fluid from the RC outlet. The working fluid then enters the HRHX (process 8 – 1) where it is heated up, reaching its maximum temperature at the HRHX outlet/ turbine inlet. The working fluid re-enters the turbine and the processes are repeated.

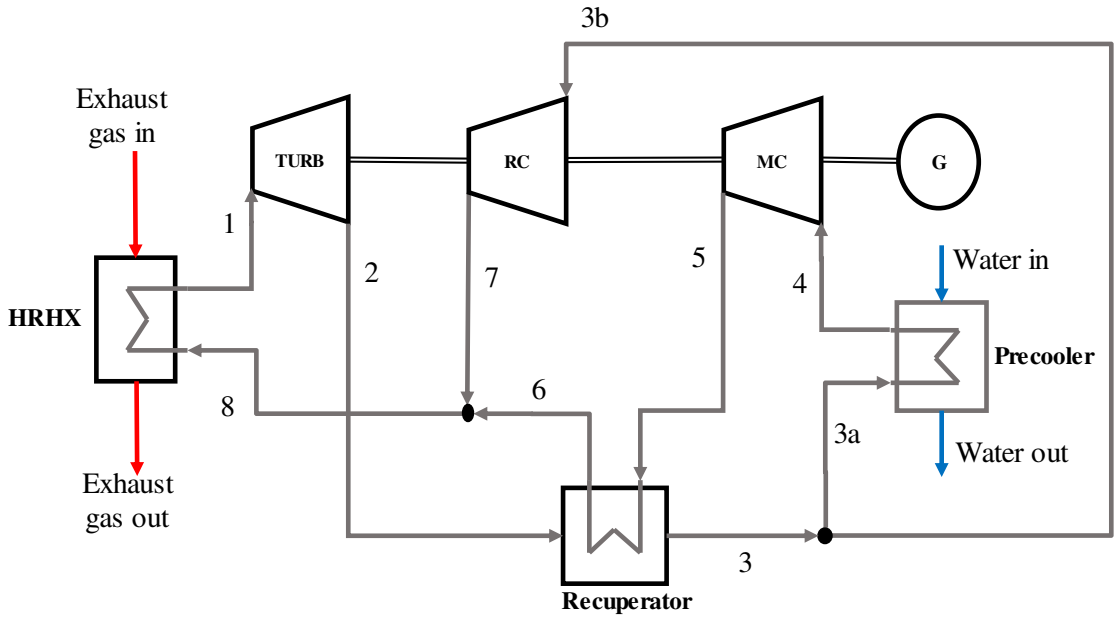


Figure 2: Schematic diagram of the single recuperator recompression s-$CO_2$ closed Brayton cycle to recover waste heat from industrial process to generate electrical power

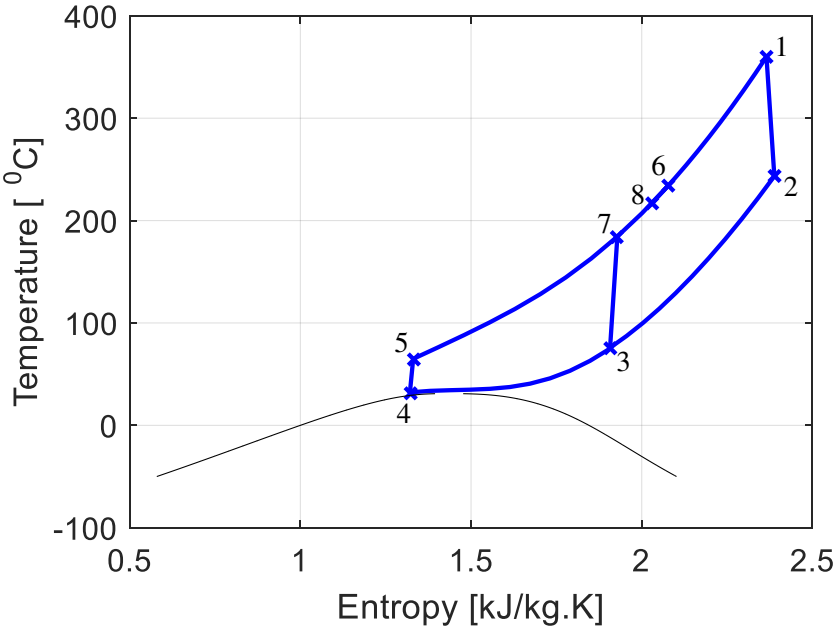


Figure 3: T-S diagram of the single recuperator recompression s-$CO_2$ closed Brayton cycle

# 3 Dynamic model development

This section presents the first principle dynamic model of the components of the s$CO_2$ closed Brayton cycle for industrial WHR. In order to study the transient performance of the WHR/s$CO_2$ plant and its control system, a dynamic model of the whole system needs to be developed. The modelled components include heat exchanger, duct, turbine, compressor, rotating shaft with generator, control valves and actuator, and PID controllers. The models are based on mass and energy conservation equations as well as other constitutive equations. The compressors and turbine are modelled by employing performance characteristic maps for the prediction of the efficiency and pressure ratio. In this work, the equations are implemented in Matlab®/Simulink® modelling platform. NIST Refprop (version 9.1) program is

used to calculate the thermo-physical properties of the fluids. The model is modular, incorporating each component model as a module. The complete cycle model is developed in Simulink® by linking together the individual component modules according to their inter-relationship as shown in Figure 4. Firstly, a Matlab® script is run to initialise the dynamic model at the design operating point. The Matlab® script loads the fluid property table, performs design point heat balance calculation and sets the component modelling parameters such as heat transfer coefficients, friction coefficients and valve coefficients.

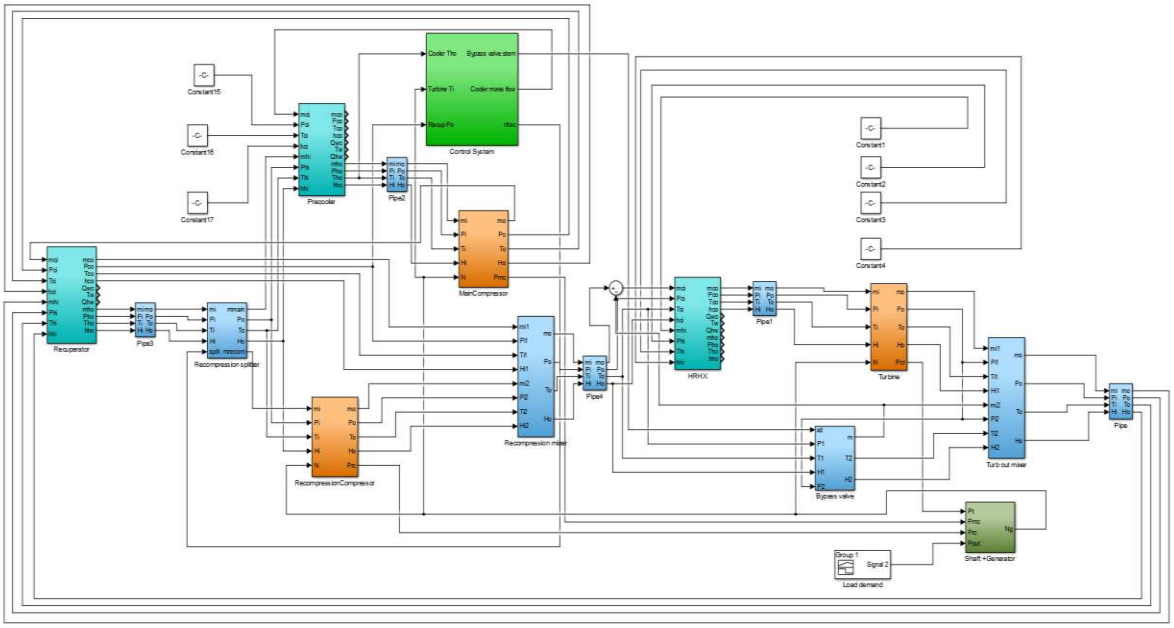


Figure 4: Component models integration in Simulink® environment

## 3.1 Heat exchanger model

The heat exchanger model is used to represent the dynamics of the HRHX, recuperator and precooler. For modelling purpose, the heat exchangers are considered as counter-flow heat exchangers consisting of three regions namely the hot stream, the cold stream and the metal wall. Mass, energy and simplified momentum conservation equations are used to model the hot and cold streams region while the separating metal wall is modelled with energy conservation equation.

The general conservation of mass equation for the hot and cold stream control volume is:

$$V\frac{d\rho}{dt} = \dot{m}_{in} - \dot{m}_{out} \tag{1}$$

The conservation of energy equation for hot stream can be expressed as:

$$V\frac{d(\rho h)}{dt} = \dot{m}_{in}h_{in} - \dot{m}_{out}h_{out} - Q_{hw} \tag{2}$$

Where $Q_{hw}$ is the convective heat transferred from the hot stream to the metal wall.

The conservation of energy equation for cold stream can be expressed as:

$$V\frac{d(\rho h)}{dt} = \dot{m}_{in}h_{in} - \dot{m}_{out}h_{out} + Q_{wc} \tag{3}$$

Where $Q_{wc}$ is the convective heat transferred from the metal wall to the cold stream.

Energy conservation equation for the metal wall can be expressed as:

$$M_w C_w \frac{dT_w}{dt} = Q_{hw} - Q_{wc} \quad (4)$$

Equations for evaluating the convective heat transferred during transient conditions are [38, 39]:

$$Q_{hw} = \kappa_{hw} \dot{m}^{\alpha} (T_h - T_w) \quad (5)$$

$$Q_{wc} = \kappa_{wc} \dot{m}^{\alpha} (T_w - T_c) \quad (6)$$

The momentum conservation equations for the hot and cold stream are simplified to a quasi-static equation of pressure loss as follows [39]:

$$P_{in} - P_{out} = \gamma \frac{\dot{m}^2}{\rho} \quad (7)$$

The pipe or duct model follows the same approach used for the hot/cold stream model but without the heat transfer term.

## 3.2 Compressor model

The rapid variation of $CO_2$ properties around the critical points makes the simulation of the compressors challenging. Therefore, the use of turbomachinery performance maps in the model is more suitable for accurately predicting the performance of the turbomachinery compared with some other methods suggested in the literature [40]. The performance characteristic maps for the compressors (and turbine) were obtained from the work of Carstens et al [41].

The most reliable way suggested for constructing a $sCO_2$ compressor map is using the approach developed for pumps [42]. Hence, the pressure rise is scaled with $U^2\rho$ while the mass flow rate is scaled with $U\rho$. $U$ is the impeller tip speed while $\rho$ is the fluid density.

Thus, the flow coefficient or scaled flow rate is given as:

$$\phi = \frac{\dot{m}}{U\rho} \quad (8)$$

The performance maps expresses the scaled pressure ratio and the compressor isentropic efficiency as functions of the flow coefficient as follows:

$$\psi = \frac{PR}{U^2\rho} = f_{maps}(\phi) \quad (9)$$

$$\eta = f_{maps}(\phi) \quad (10)$$

The compressor outlet conditions is calculated from the pressure ratio and the isentropic efficiency as follows:

$$P_{out} = P_{in}(PR) \quad (11)$$

$$h_{out} = h_{in} + \frac{h_{out,isen} - h_{in}}{\eta} \quad (12)$$

The outlet temperature is then calculated from the fluid thermodynamic property relations.

The compressor power, $P_c$, is given as:

$$P_c = \dot{m}(h_{out} - h_{in}) \quad (13)$$

## 3.3 Turbine model

The original turbine performance maps are transformed to provide relationship between pressure ratio and flow coefficient and between efficiency and flow coefficient at constant shaft speed parameter. The turbine model is similar to the compressor model. However, the $CO_2$ working fluid is considered as an ideal gas under turbine conditions. Hence, the flow coefficient is expressed as follows:

$$\phi = \frac{\dot{m}\sqrt{T_{in}}}{P_{in}} \quad (14)$$

The performance maps are used to obtain the pressure ratio and the isentropic efficiency of the turbine.

$$PR = f_{maps}(\phi, N) \quad (15)$$

$$\eta = f_{maps}(\phi, N) \quad (16)$$

Where N is the shaft rotational speed.

The turbine outlet conditions are calculated as follows:

$$P_{out} = \frac{P_{in}}{PR} \quad (17)$$

$$h_{out} = h_{in} - \eta(h_{in} - h_{out,isen}) \quad (18)$$

The power delivered by the turbine, $P_t$, is:

$$P_t = \dot{m}(h_{in} - h_{out}) \quad (19)$$

## 3.4 Rotating shaft and generator model

The turbine drives the MC, the RC and the generator on a single shaft. The turbine will exert positive torque while compressors and electric generator will exert negative torque An unbalance torque on the shaft during transient will cause the shaft to accelerate or decelerate. The transient behaviour of the shafts can be determined from the dynamic equation:

$$(J_t + J_{mc} + J_{rc} + J_{gen})N\frac{dN}{dt} = (P_t - P_{mc} - P_{rc} - P_{gen} - P_{loss}) \quad (20)$$

Where J represents the component inertias.

The power delivered to the generator can be determined from the electric load demand, $P_{load}$, and the generator efficiency, $\eta_{gen}$:

$$P_{gen} = \frac{P_{load}}{\eta_{gen}} \quad (21)$$

## 3.5 Control valve and actuator model

Valves are used for flow control in the cycle or for throttling flow to a desired pressure. Mass and energy storage in a control valve can be considered negligible. The mass flow rate through the valve, $\dot{m}$, is dependent on the valve's upstream and downstream pressure, $P_{in}$ and $P_{out}$, on the incoming fluid density, $\rho_{in}$, and on the fractional valve opening, $y$ [43]:

$$\dot{m} = C_v y \sqrt{P_{in}\rho_{in}\left(1 - {}^{P_{out}}/_{P_{in}}\right)} \qquad (22)$$

Where $C_v$ is the constant valve construction coefficient.

The fractional valve opening or flow area,$y$, is defined as the ratio of valve's current flow area to its flow area when fully open. It will depend on the valve stem position, $x$, (also referred to as valve travel) and the valve flow characteristic dictated by the geometry of the valve. The valve travel position is usually determined by the actuator based on the signal from the controller. The actuator will drive the valve stem position, $x$, to its demanded position, $x_d$, specified by the controller output signal. It will take a certain amount of time for the actuator to move the stem position to the demanded value. Hence, the dynamics of the actuator plus valve can be modelled with a first order exponential lag as follows:

$$\tau \frac{dx}{dt} = x_d - x \qquad (23)$$

Where $\tau$ is the time constant associated with the actuator and $x_d$ is the demanded valve travel.

## 3.6 PID controller model

The PID (Proportional-Integral-Derivative) controllers are designed to act on the error signals to produce the control signals. The general function of the controller is to keep the controlled variable near its desired value. The control action of a PID is defined as [39]:

$$u(t) = K_p e(t) + K_i \int_0^t e(t)\, d\tau + K_d \frac{de(t)}{dt} \qquad (3\text{-}24)$$

Where $K_p$ is the proportional gain, $K_i$ is the integral gain and $K_d$ is the derivative gain.

The three gains are the tuning parameters for the controller. The control signal, $u(t)$, is the summation of the three function of error, $e(t)$, from a specified set point. Proportional control has the effect of increasing the loop gain to make the system less sensitive to load disturbances, the integral of error is used to eliminate steady state error and the derivative term helps to improve closed loop stability.

## 3.7 Steady state verification of component models and dynamic model validation

The suitability of the Matlab/Simulink model for predicting the performance of the cycle components at steady state was verified by comparing the simulation results of component models with value obtained from Kim et al [13] for a $sCO_2$ closed Brayton cycle. Comparison of the simulation results at steady state with the literature values is presented in Table 1. The steady state predictions of the components models were found to agree well with the literature data. The maximum relative difference is about 0.25%.

316 Table 1: Comparison of the components simulation values at steady state with literature value obtained
317 from Kim et al [13]

| Parameters | Literature value | Simulation value | Relative difference |
|---|---|---|---|
| **Compressor:** | | | |
| Inlet pressure (bar) | 77 | 77 | 0 |
| Inlet temperature ($^0$C) | 32 | 32 | 0 |
| Outlet pressure (bar) | 200 | 200 | 0 |
| Outlet temperature ($^0$C) | 61 | 60.81 | 0.3% |
| Specific work (kJ/kg) | 20.3 | 20.29 | 0.05% |
| **Turbine:** | | | |
| Inlet pressure (bar) | 200 | 200 | 0 |
| Inlet temperature ($^0$C) | 600 | 600 | 0 |
| Outlet pressure (bar) | 77 | 77 | 0 |
| Outlet temperature ($^0$C) | 482 | 482.19 | 0.04% |
| Specific work (kJ/kg) | 133.4 | 133.37 | 0.02% |
| **Heat source:** | | | |
| Inlet temperature ($^0$C) | 360 | 360.54 | 0.15% |
| Outlet temperature ($^0$C) | 600 | 600 | 0 |
| Specific heat input (kJ/kg) | 295.7 | 295.21 | 0.17% |
| **Recuperator:** | | | |
| Temperature in, hot/cold ($^0$C) | 482/61 | 482.19/60.81 | 0.04/0.3% |
| Temperature out, hot/cold ($^0$C) | 76/360 | 75.81/360.54 | 0.25/0.15% |
| Specific heat transferred (kJ/kg) | 475.2 | 475.66 | 0.1% |
| **Precooler:** | | | |
| Inlet temperature ($^0$C) | 76 | 75.81 | 0.25% |
| Outlet temperature ($^0$C) | 32 | 32 | 0 |
| Specific heat transferred (kJ/kg) | 182.6 | 182.13 | 0.26% |

318

319 At this stage, there is no plant data for validating the dynamic model of the single recuperator
320 recompression $sCO_2$ cycle. However, dynamic model validation of a simple $tCO_2$ cycle was carried out
321 using experimental data from a kW-scale test bench for WHR from exhaust gas of diesel engine [26].
322 It should be noted that the test bench did not have a turbine; an expansion valve is used instead. Also,
323 a reciprocating plunger pump is used to circulated the $CO_2$ fluid in the cycle. The pump rotational speed
324 was reduced from 110 rpm to 60 rpm in steps as shown in Figure 5(a). The model was validated with
325 data of dynamic responses to changes in the pump rotational speed. Validation results are shown for the
326 $CO_2$ mass flow rate and $CO_2$ temperature at gas heater outlet temperature in Figure 5(b) and (c)
327 respectively. The Simulink® model was found to give good predictions of the profile of the $CO_2$ mass
328 flow and gas heater outlet temperature. The noticed differences between the experimental data and the
329 simulation results can be attributed to uncertainties with respect to the design and operational
330 parameters of the test bench. For instance, pump displacement, efficiency, off-design performance data
331 and gas heater size are not known. All of these were assumed in the Simulink® model.

332

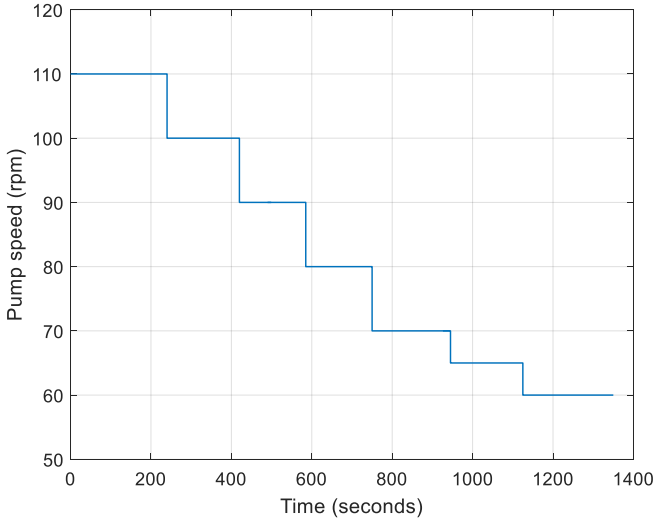


(a) Pump rotational speed

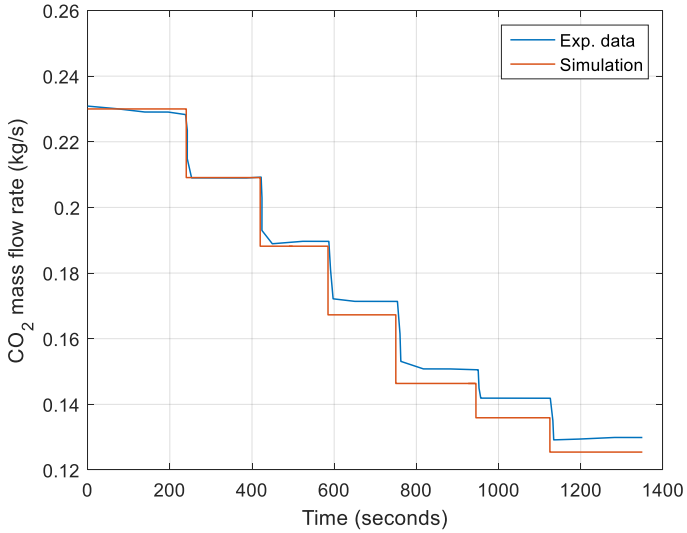


(b) $CO_2$ mass flow rate - experimental data versus simulation result

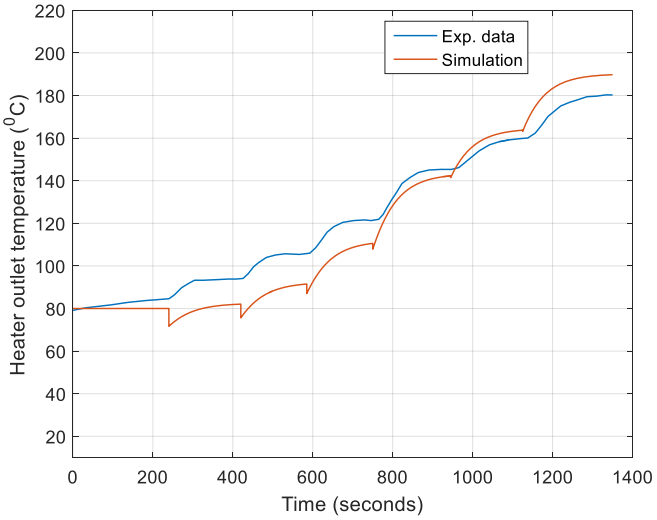


(c) Gas heater outlet temperature – experimental data versus simulation result

Figure 5 Model validation with experimental data from test bench

# 4 Control strategy

The overall control structure for the $sCO_2$ closed Brayton cycle for WHR application is shown in Figure 6. Control systems are essential in order to achieve stable operation, optimal performance and net power output under fluctuating waste heat source conditions. PID feedback control methods are adopted for the controllers and the control strategy is implemented in Simulink®. PID controller is the most commonly used controller in industrial processes due to the uncomplicated principle of operation, simple structure and ruggedness [32].

The non-ideal behaviour of the $CO_2$ working fluid around the critical point poses unique challenges not seen in other cycles like the ORC and SRC. The rapid fluid density changes around the critical point is illustrated in Figure 7. Therefore, maintaining a fixed inlet conditions for the main compressor is an important objective of the control systems. Hence, the main compressor inlet/precooler outlet temperature and pressure are selected as controlled variables. The feedback control of the cooling water controller (CWC) serves to keep the main compressor inlet temperature at the set value (Figure 6). This is achieved by manipulating the mass flow rate of the cooling water. On the other hand, the throttle valve, V2, is regulated to keep the compressors inlet pressure at the design values.

Another variable chosen to be controlled is the turbine inlet temperature, in case this is required. This is controlled primarily by the feedback control loop for the bypass valve controller (BVC). The bypass control valve, V1, is located between the HRHX inlet and turbine outlet to divert part of the working fluid from the HRHX and turbine (Figure 6). The measured turbine inlet temperature is compared with the set point value. The bypass valve controller then uses the error to produce a control signal based on the PID algorithm. The control signal is sent to the bypass valve actuator to manipulate the valve stem position and thus the opening and closing of the bypass valve.

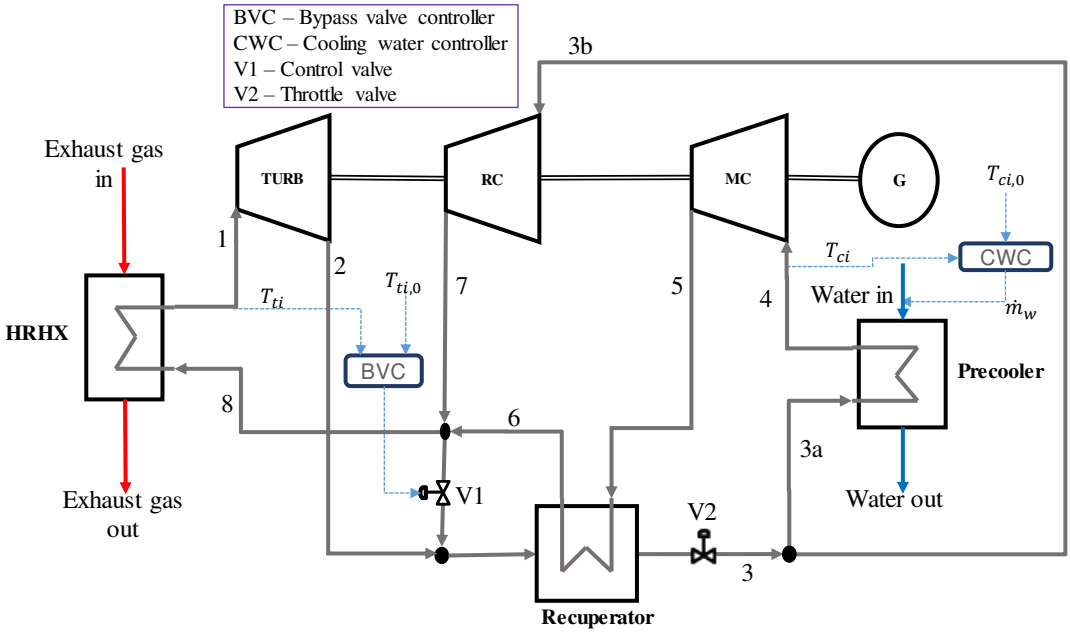


Figure 6: Overall control scheme for the WHR $sCO_2$ power cycle system

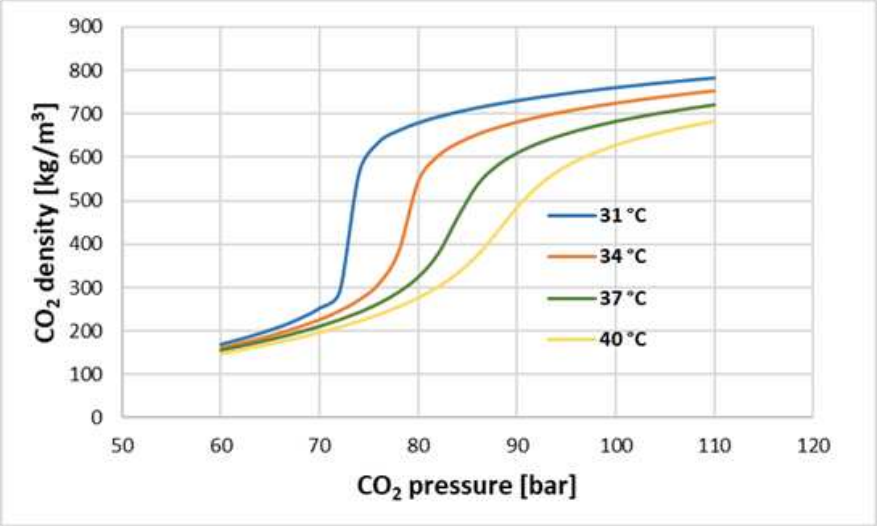


Figure 7: $CO_2$ density variation in the critical condition region

# 5 Results and discussion

## 5.1 Steady state simulation results and preliminary sizing of heat exchangers

The steady state calculation and heat exchanger design is carried out by adopting an integrated approach, which allows for cycle's heat balance calculation and heat exchanger preliminary design to be performed simultaneously. This offers the advantage of a more accurate performance calculation for the system because the heat exchanger pressure losses will be based on actual values from results of heat exchanger design and not on assumed values, as is usually done. The codes were implemented in Matlab programming environment. It is linked with Refprop (version 9.1) program as an external function for the calculation of the thermo-physical properties of the fluids. Detailed description of the steady state thermodynamic performance calculation and heat exchanger design methodology can be found in the work of Olumayegun et al. [44].

The results of the steady state simulation and heat exchanger design calculations provide the physical parameters of the components as well as the initial values for the dynamic performance simulation of the system.

### 5.1.1 Results of steady state simulation at design point

In this study, the upper boundary of waste heat fluctuation (maximum mass flow rate and maximum temperature) is adopted as the design point for the WHR system. Therefore, the system will operate at either design point or mass flow rate and temperature below the design point. The main design specification, system parameters and assumptions for steady state performance calculation are as follows:

- The case of exhaust waste heat gas from cement industry at a flow rate of 100 kg/s and temperature of 380 $^0$C is considered [6]
- HRHX terminal temperature difference is selected as 20 $^0$C. Hence, the heated $CO_2$ leaves the HRHX and enters the turbine temperature at 360 $^0$C
- The precooler cooling stream is water at 22 $^0$C
- The temperature and pressure of the working fluid at precooler outlet is set just above the critical point for the benefit of reduced compression work. Hence, the precooler outlet get cooled to 32 $^0$C at a corresponding optimum pressure of 79 bar
- The maximum cycle pressure at outlet of main compressor is set at 250 bar
- The recuperator terminal temperature difference is 10 $^0$C

- The isentropic efficiency of the turbine, main compressor and recompression compressor are set at 90%, 89% and 88% respectively
- The heat and pressure losses in the connecting ducts/pipes are assumed to be negligible

Table 2 list the state point simulation results of the WHR $sCO_2$ power cycle (refer to Figure 2 for the numbering of the state points). The results of steady state design point performance of the system is presented in Table 3. About 15 MW of heat is recovered from the exhaust gas and the electric power generated is about 5 MWe. This amount to efficiency of about 33% for the WHR $sCO_2$ system.

Table 2: Results of steady state simulation of the $sCO_2$ WHR system

| State | m (kg/s) | P (bar) | T ($^0$C) | h (kJ/kg) |
|---|---|---|---|---|
| 1 | 80.40 | 249.87 | 360 | 794.47 |
| 2 | 80.40 | 80.44 | 243.37 | 688.62 |
| 3 | 80.40 | 79.64 | 74.95 | 484.31 |
| 3a | 53.98 | 79.64 | 74.95 | 484.31 |
| 3b | 26.42 | 79.64 | 74.95 | 484.31 |
| 4 | 53.98 | 79 | 32 | 298.78 |
| 5 | 53.98 | 250 | 64.95 | 325.91 |
| 6 | 53.98 | 249.87 | 233.37 | 630.21 |
| 7 | 26.42 | 249.87 | 166.24 | 541.40 |
| 8 | 80.40 | 249.87 | 216.71 | 606.98 |

Table 3: Results of steady state thermodynamic performance of the WHR system

| Parameters | Value |
|---|---|
| Waste heat recovered | 15.07 MW |
| Turbine power | 8.51 MW |
| Main compressor power | 1.46 MW |
| Recompression compressor power | 1.99 MW |
| Recuperator duty | 16.43 MW |
| Precooler duty | 10.01 MW |
| HRHX effectiveness | 88.21% |
| Recuperator effectiveness | 95.71% |
| Precooler effectiveness | 80.33% |
| Cooling water flow rate | 104.48 kg/s |
| Optimum recompression fraction | 0.33 |
| Net power output | 5 MW |
| Efficiency | 33.13 |

### 5.1.2 Results of preliminary sizing of heat exchangers

In the $sCO_2$ power cycle, the size of the turbine and the compressors are very small compared to the heat exchangers, hence, the system dynamic performance is mainly determined by the heat exchangers. The volume of $CO_2$ in the heat exchangers, the heat exchanger material properties and the thermal mass between the working fluid and the exhaust gas will influence the transient behaviour of the WHR system. Therefore, preliminary sizing was performed for the HRHX, recuperator and precooler. Essentially, preliminary sizing entails determining the surface area, volume, length, metal wall mass, internal temperature profiles and pressure losses of the heat exchangers. The heat exchangers were assumed to be Printed Circuit Heat Exchanger (PCHE) type [44].

Table 4 shows the result of the preliminary sizing of the heat exchangers. The hot and cold stream temperature profile from the heat exchanger inlet to the outlet is given in Figure 8. Figure 8a indicates efficient matching of the temperature profile of the $CO_2$ working fluid and the exhaust gas in the HRHX. Unlike the evaporator/boiler of ORC and SRC, there is no pinch point limitation in the HRHX because $CO_2$ does not undergo any phase change. Figure 8b shows that optimum selection of split fraction (or recompression fraction) allows the recuperator cold stream to be preheated as high as possible without risk of pinch point developing in the recuperator. Figure 8c shows the precooler temperature profile. Among the cycle components, the precooler operates closest to the critical region. The specific heat capacity of $CO_2$ increases rapidly in the critical region, hence, the unusual temperature profile and occurrence of pinch point in the precooler. Precooler heat transfer is nearly a two-phase condensation process with constant temperature in some section of the precooler.

Table 4: Heat exchanger sizing results for the HRHX, recuperator and precooler

| **Description** | **HRHX** | **Recuperator** | **Precooler** |
|---|---|---|---|
| Heat transfer duty (MW) | 15.07 | 16.42 | 10.01 |
| Fluid, hot side/cold side | Flue gas/$CO_2$ | $CO_2$/$CO_2$ | $CO_2$/Water |
| Number of modules | 14 | 8 | 2 |
| Surface area ($m^2$) | 8997.79 | 8297.96 | 1442.50 |
| Thermal density ($MW/m^3$) | 1.2 | 1.4 | 4.95 |
| Hot side pressure loss (kPa) | 10 | 80 | 67 |
| Cold side pressure loss (kPa) | 0.4 | 13 | 6 |
| Total core volume ($m^3$) | 12.60 | 11.62 | 2.02 |
| Total core mass (kg) | 56829 | 52418 | 9253 |

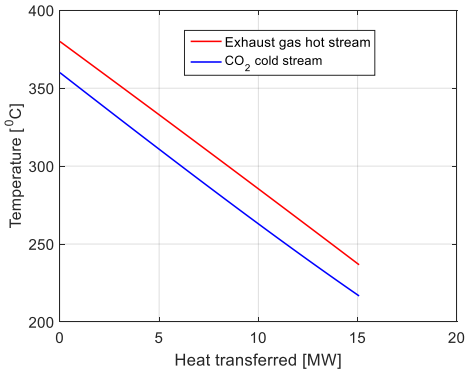


(a) HRHX temperature profile

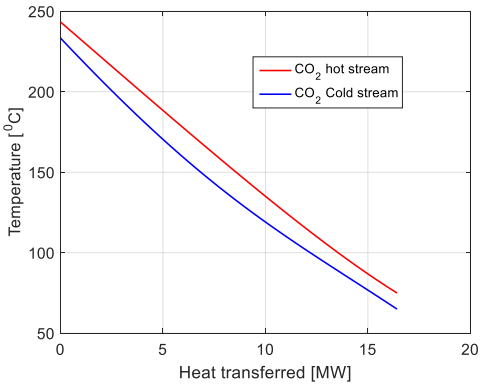


(b) Recuperator temperature profile

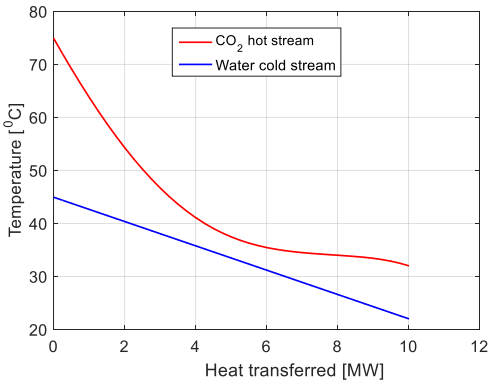


(c) Precooler temperature profile

Figure 8: Hot and cold stream temperature profile for the (a) HRHX (b) recuperator and (c) Precooler

## 5.2 Open loop response simulation

Open loop simulation of the system was performed to investigate the dynamic behaviour without any control action. Dynamic response to step change in the temperature of the waste heat source was observed. Step change in exhaust gas temperature from the design value of 380 $^0$C to 300 $^0$C was applied at time equal to 100 seconds. Figure 9 shows the open loop transient responses of some of the system variables. The turbine inlet temperature as well as the MC inlet temperature is seen to drop from the steady state value (Figure 9a). Reduced exhaust gas temperature means that working fluid cannot be heated to the design values. The power delivered by the turbine is reduced due to the reduced inlet temperature and operation of the turbine at off-design condition. However, the power consumed by the compressors are increased as the compressors are now operating at conditions different from the design point value. Hence, the net power output is reduced significantly, to almost zero. Also at off-design condition, the turbine outlet pressure increases. If this high pressure is fed back to the compressor inlet, coupled with the changes in compressor inlet temperature, the compressor outlet pressure will again increase. This could lead to a form of positive feedback, thus making the system unstable. As seen in Figure 9c, the compressor outlet pressure of about 400 bar is not permissible. Hence, control system has to be implemented for stable and safe operation of the plant.

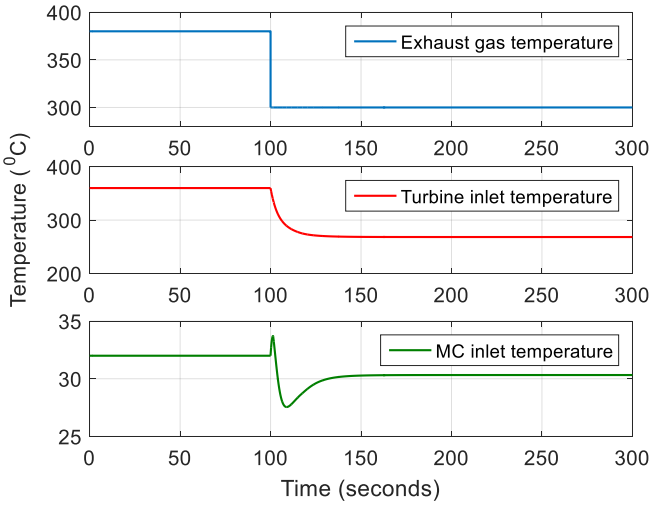


(a) Step change in exhaust gas temperature and open loop transient responses of turbine inlet temperature and MC inlet temperature

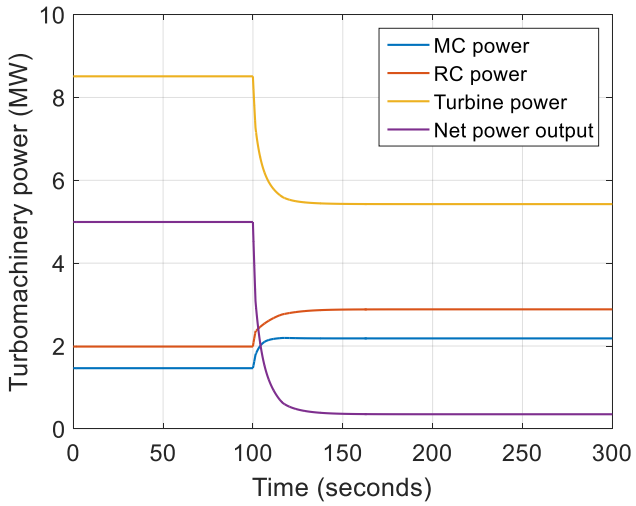


(b) Open loop responses of turbomachinery power and the net power output

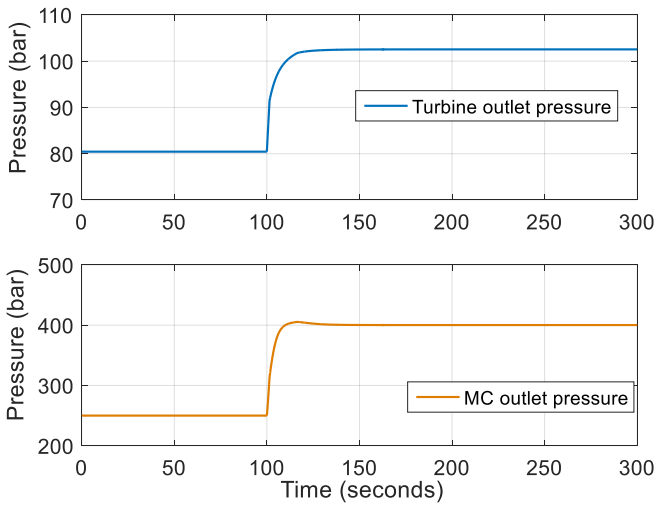


(c) Open loop responses of turbine inlet pressure and MC outlet pressure

459 Figure 9: Results of system open loop responses under step change in exhaust gas temperature

## 5.3 Dynamic simulation under fluctuating mass flow rate of waste heat source

In this section, the system dynamic response to change in exhaust gas mass flow rate between 100 kg/s and 50 kg/s is simulated to study the transient behaviour and control strategy for the plant under fluctuating mass flow rate of waste heat. The dynamic response of the plant with implementation of cooling water control and throttle valve regulation is shown in Figure 10. The cooling water controller acts to maintain the MC inlet temperature at 32 $^0$C while the throttle valve is regulated to keep the MC inlet pressure at 79 bar. Figure 10b shows that by adjusting the water flow rate, the MC inlet temperature is kept within 0.4 $^0$C of the steady state value. Consequently, the power consumed by the compressor remain almost constant during the transient (Figure 10d). However, reduction in the exhaust gas mass flow rate while the CO2 flow rate remain constant means that the turbine inlet temperature and power delivered by the turbine will drop from the design point value (Figure 10c and Figure 10d).

Bypass valve controller is added to investigate the effect of maintaining a fixed turbine inlet on the transient performance of the plant. The bypass valve controller is engaged to maintain the turbine inlet temperature at 360 $^0$C. Results of dynamic simulation is shown in Figure 11. As the bypass valve is opened, the amount of $CO_2$ flowing through the HRHX and turbine is reduced in order to maintain the turbine inlet temperature at the set point (Figure 11a). The reduced mass flow rate of $CO_2$ leads to reduced heat recovery in the HRHX and large reduction in power delivered by the turbine. Hence, huge drop in net power output compared to the previous case of no bypass valve control. It is found that with bypass valve control, the possible range of variation of exhaust gas mass flow rate is restricted to between 100% and 70% of the design value (Figure 11a) because exhaust gas mass flow rate below 70% of design value results in zero net power output (Figure 11d). It can be concluded that maintaining a constant turbine inlet temperature at the expense of mass flow rate is not beneficial for the WHR system. The temperature of the exhaust gas exiting the HRHX is seen to increase during the transient such that less waste heat is recovered (Figure 11c).

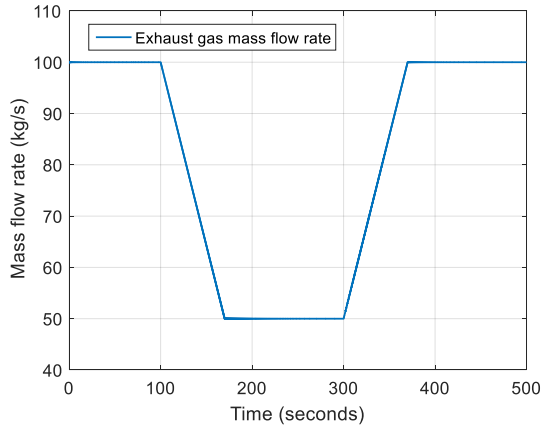


(a) Simulated fluctuating mass flow rate of waste heat source

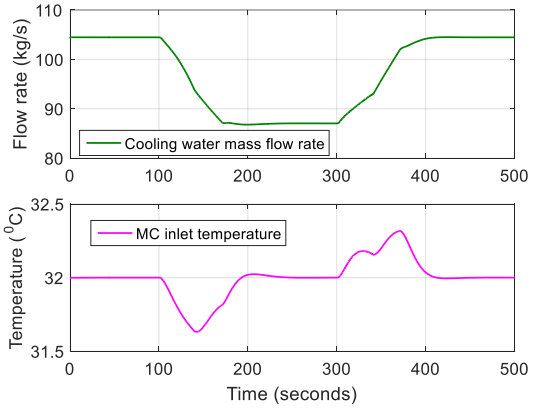


(b) Dynamic response of cooling water flow rate and MC inlet temperature

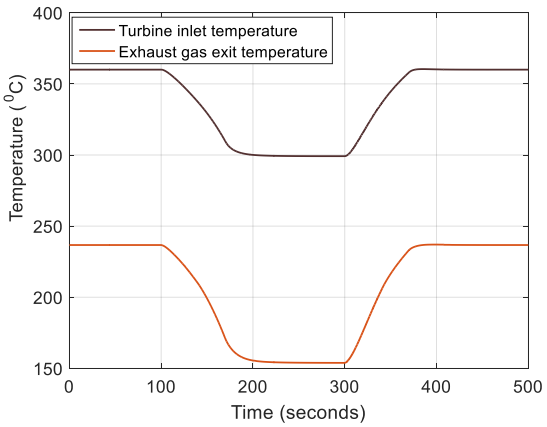


(c) Dynamic response of turbine inlet temperature and exhaust gas exit temperature from HRHX

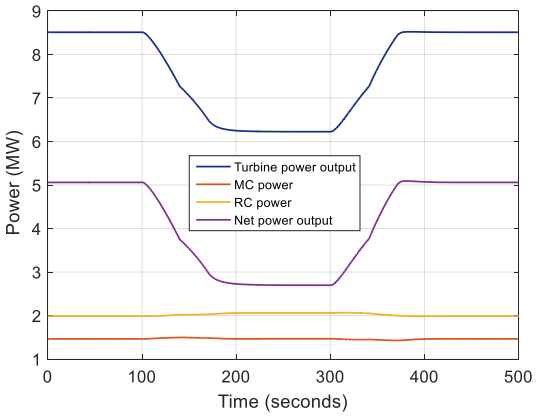


(d) Dynamic response of turbomachinery power and net power output

Figure 10: Results of dynamic simulation under fluctuating mass flow rate of waste heat source with cooling water controller and throttle valve regulation to maintain a fixed main compressor inlet condition

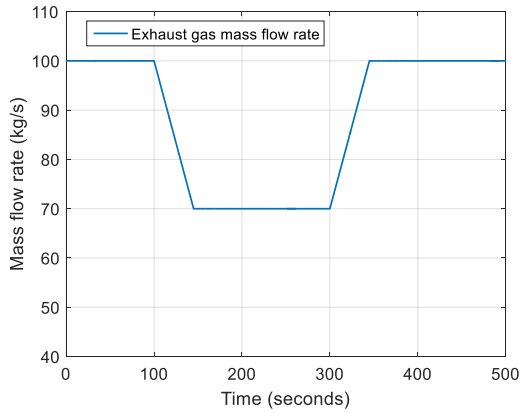


(a) Simulated fluctuating mass flow rate of waste heat source

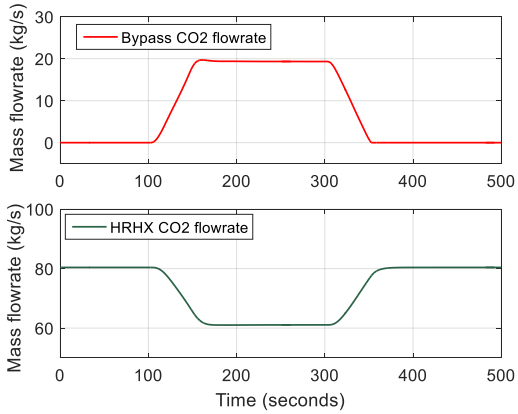


(b) $CO_2$ mass flow rate through the bypass valve and through the HRHX-turbine

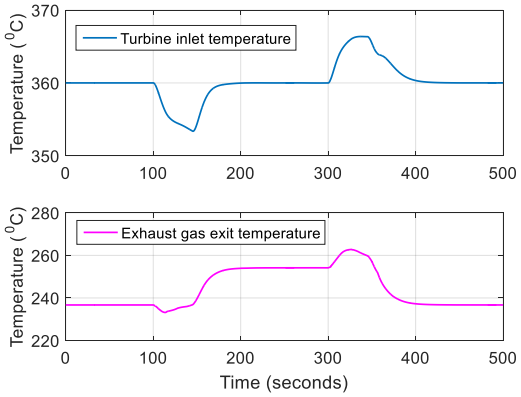


(c) Dynamic response of turbine inlet temperature and exhaust gas exit temperature

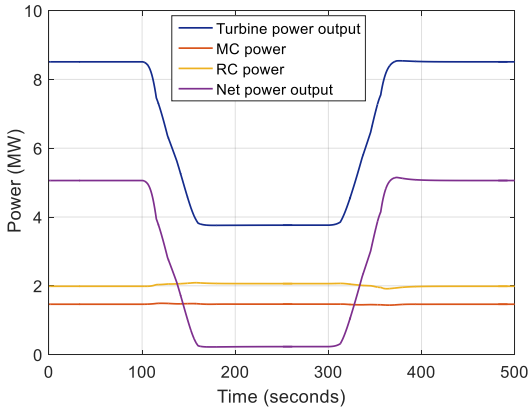


(d) Dynamic response of the turbomachinery power and net power output

Figure 11: Results of dynamic simulation under fluctuating mass flow rate of waste heat source with bypass valve control to maintain fixed turbine inlet temperature

## 5.4 Dynamic simulation under fluctuating temperature of waste heat source

Exhaust gas temperature variation between 380 $^0$C and 300 $^0$C is simulated to study the dynamic response of the WHR system during fluctuation of waste heat temperature. Similar to section 5.3, cooling water controller is used to maintain MC inlet temperature at 32 $^0$C while throttle valve regulator keeps the MC inlet pressure at 79 bar. Some results of the system dynamic simulation are presented in Figure 12. The change in turbine inlet temperature is seen to follow the change in exhaust gas temperature (Figure 12a). The cooling water controller is able to keep the MC inlet temperature to within 0.06 0C of the set point value (Figure 12b). Reduced turbine inlet temperature results in reduce turbine power and consequent reduction in net power output as shown in Figure 12c. However, significant improvement in off-design net power output is noticed compared to the open loop case. The loss in net power output is only about 2.8 MW compared to about 4.8 MW under open loop simulation.

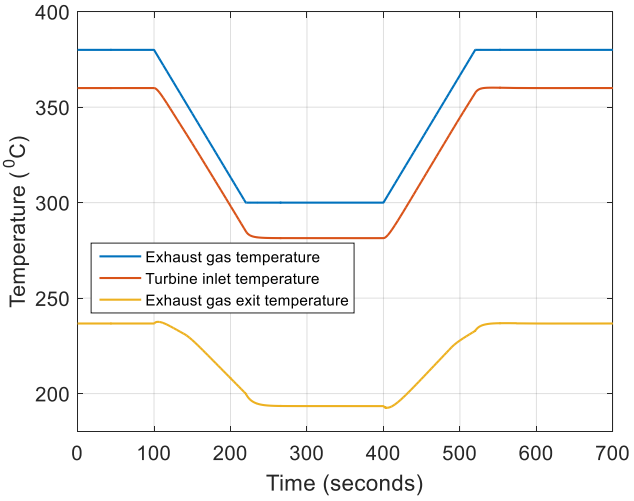


(a) Simulated fluctuating temperature of waste heat source and dynamic responses of turbine inlet and exhaust gas exit temperature

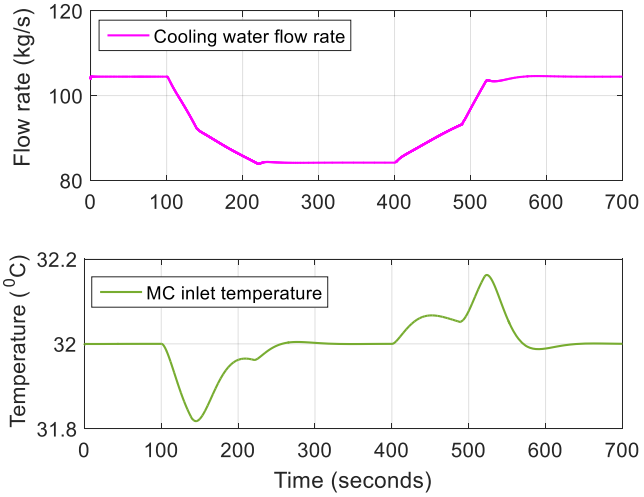


(b) Dynamic responses of cooling water mass flow rate and MC inlet temperature

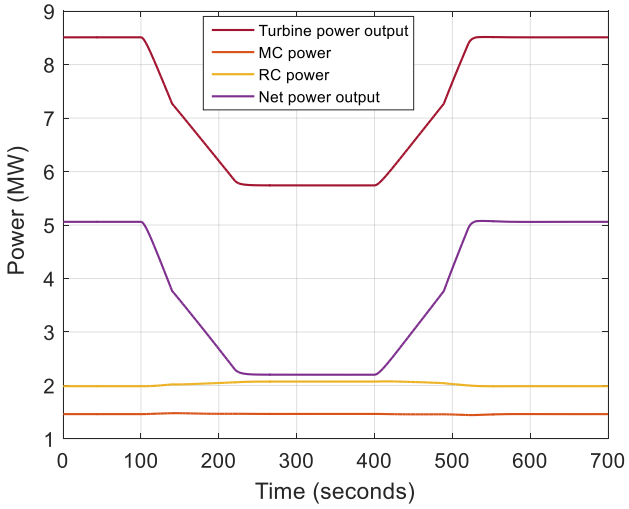


(c) Dynamic responses of turbomachinery power and net power output

Figure 12: Results of dynamic simulation under fluctuating temperature of waste heat source with cooling water controller and throttle valve regulation to maintain a fixed main compressor inlet condition

# 6 Conclusions

In this paper, dynamic modelling and design of PID based control systems for single recuperator recompression $sCO_2$ closed Brayton cycle for industrial WHR application were reported. To obtain design point values and parameters for the dynamic model, steady state simulation and preliminary sizing of the heat exchangers were carried out for the case of exhaust gas from cement industry at a flow rate of 100 kg/s and temperature of 380 $^0$C. The dynamic model was developed in Matlab/Simulink environment to predict system transient and to test control strategies for changes in exhaust gas mass flow rate and temperature operation. Based on this, the dynamic performance of the system under fluctuating waste heat source mass flow rate and temperature was analysed. The main conclusions of this work can be summarised as follows:

- The steady state thermodynamic analysis at design point conditions of the proposed single-recuperator recompression $sCO_2$ cycle predicted a thermal efficiency of about 33%.
- Preliminary design of the heat exchanges confirmed the efficient matching of the temperature profile of the $CO_2$ working fluid and the exhaust gas in the gas heater
- Open loop step response test highlights the need to maintain fixed working fluid pressure and temperature at precooler outlet/MC inlet.
- Cooling water control was used to keep MC inlet temperature at design value during transient. Throttle valve regulation was used to maintain a constant compressor inlet pressure. These control strategies were able to achieve stable operation of the system.
- Results of dynamic simulation and control system implementation indicates that it is better to allow the turbine inlet temperature to vary according to the waste heat source condition (i.e. maintain a constant flow rate of $CO_2$). Therefore, between the choice of constant turbine inlet temperature and constant turbine mass flow rate, constant mass flow rate is more beneficial because more waste heat can be recovered during transient variation of flue gas condition.

In view of these findings, the single recuperator recompression $sCO_2$ cycle investigated in this work could be a promising power conversion system for WHR from industrial processes. In addition, this study shows that dynamic modelling and simulation of the system could contribute to the understanding of the dynamic characteristics and control strategies for operation of the plant under fluctuating waste heat source condition.

# Acknowledgement

The authors would like to acknowledge GE Power UK for financial support of this research.

# References

[1] T. Brown, A. Gambhir, N. Florin, and P. Fennell, "Reducing $CO_2$ emissions from heavy industry: a review of technologies and considerations for policy makers," Briefing Paper No 7, Grantham Institute for Climate Change, Imperial College London, 2012.

[2] S. Khurana, R. Banerjee, and U. Gaitonde, "Energy balance and cogeneration for a cement plant," *Applied Thermal Engineering,* vol. 22, no. 5, pp. 485-494, 2002.

[3] J. Wang, Y. Dai, and L. Gao, "Exergy analyses and parametric optimizations for different cogeneration power plants in cement industry," *Applied Energy,* vol. 86, no. 6, pp. 941-948, 2009.

[4] C. Carcasci and L. Winchler, "Thermodynamic Analysis of an Organic Rankine Cycle for Waste Heat Recovery from an Aeroderivative Intercooled Gas Turbine," *Energy Procedia,* vol. 101, pp. 862-869, 2016.

[5] H. Chen, D. Y. Goswami, and E. K. Stefanakos, "A review of thermodynamic cycles and working fluids for the conversion of low-grade heat," *Renewable and Sustainable Energy Reviews,* vol. 14, no. 9, pp. 3059-3067, 2010.

[6] O. A. Oyewunmi, S. Ferré-Serres, S. Lecompte, M. van den Broek, M. De Paepe, and C. N. Markides, "An Assessment of Subcritical and Trans-critical Organic Rankine Cycles for Waste-heat Recovery," *Energy Procedia,* vol. 105, pp. 1870-1876, 2017.
[7] Z. Li, X. He, Y. Wang, B. Zhang, and H. He, "Design of a flat glass furnace waste heat power generation system," *Applied Thermal Engineering,* vol. 63, no. 1, pp. 290-296, 2014.
[8] Ö. Kaşka, "Energy and exergy analysis of an organic Rankine for power generation from waste heat recovery in steel industry," *Energy Conversion and Management,* vol. 77, pp. 108-117, 2014.
[9] X. Zhang, L. Wu, X. Wang, and G. Ju, "Comparative study of waste heat steam SRC, ORC and S-ORC power generation systems in medium-low temperature," *Applied Thermal Engineering,* vol. 106, pp. 1427-1439, 2016.
[10] G. Yu, G. Shu, H. Tian, Y. Huo, and W. Zhu, "Experimental investigations on a cascaded steam-/organic-Rankine-cycle (RC/ORC) system for waste heat recovery (WHR) from diesel engine," *Energy Conversion and Management,* vol. 129, pp. 43-51, 2016.
[11] J. G. Andreasen, A. Meroni, and F. Haglind, "A comparison of organic and steam Rankine cycle power systems for waste heat recovery on large ships," *Energies,* vol. 10, no. 4, p. 547, 2017.
[12] M. Pasetti, C. M. Invernizzi, and P. Iora, "Thermal stability of working fluids for organic Rankine cycles: An improved survey method and experimental results for cyclopentane, isopentane and n-butane," *Applied Thermal Engineering,* vol. 73, no. 1, pp. 764-774, 2014.
[13] Y. M. Kim, C. G. Kim, and D. Favrat, "Transcritical or supercritical CO2 cycles using both low- and high-temperature heat sources," *Energy,* vol. 43, no. 1, pp. 402-415, 2012.
[14] Y. Chen, W. Pridasawas, and P. Lundqvist, "Dynamic simulation of a solar-driven carbon dioxide transcritical power system for small scale combined heat and power production," *Solar Energy,* vol. 84, no. 7, pp. 1103-1110, 2010.
[15] L. Li, Y. Ge, X. Luo, and S. A. Tassou, "Experimental investigation on power generation with low grade waste heat and CO2 transcritical power cycle," *Energy Procedia,* vol. 123, pp. 297-304, 2017.
[16] J. Sarkar, "Review and future trends of supercritical CO2 Rankine cycle for low-grade heat conversion," *Renewable and Sustainable Energy Reviews,* vol. 48, pp. 434-451, 2015.
[17] O. Olumayegun, M. Wang, and G. Kelsall, "Closed-cycle gas turbine for power generation: A state-of-the-art review," *Fuel,* vol. 180, no. 0, pp. 694-717, 2016.
[18] S. Karellas, A. D. Leontaritis, G. Panousis, E. Bellos, and E. Kakaras, "Energetic and exergetic analysis of waste heat recovery systems in the cement industry," *Energy,* vol. 58, pp. 147-156, 2013.
[19] Y. Chen, P. Lundqvist, A. Johansson, and P. Platell, "A comparative study of the carbon dioxide transcritical power cycle compared with an organic rankine cycle with R123 as working fluid in waste heat recovery," *Applied Thermal Engineering,* vol. 26, no. 17, pp. 2142-2147, 2006.
[20] E. Cayer, N. Galanis, M. Desilets, H. Nesreddine, and P. Roy, "Analysis of a carbon dioxide transcritical power cycle using a low temperature source," *Applied Energy,* vol. 86, no. 7, pp. 1055-1063, 2009.
[21] X. Wang and Y. Dai, "Exergoeconomic analysis of utilizing the transcritical CO2 cycle and the ORC for a recompression supercritical CO2 cycle waste heat recovery: A comparative study," *Applied Energy,* vol. 170, pp. 193-207, 2016.
[22] S. Mondal and S. De, "CO2 based power cycle with multi-stage compression and intercooling for low temperature waste heat recovery," *Energy,* vol. 90, pp. 1132-1143, 2015.
[23] G. Shu, L. Shi, H. Tian, X. Li, G. Huang, and L. Chang, "An improved CO2-based transcritical Rankine cycle (CTRC) used for engine waste heat recovery," *Applied Energy,* vol. 176, pp. 171-182, 2016.
[24] S. Banik, S. Ray, and S. De, "Thermodynamic modelling of a recompression CO2 power cycle for low temperature waste heat recovery," *Applied Thermal Engineering,* vol. 107, pp. 441-452, 2016.
[25] O. Olumayegun, "Study of closed-cycle gas turbine for application to small modular reactors (SMRs) and coal-fired power generation through modelling and simulation," PhD Thesis,

Department of Chemical and Biological Engineering, The University of Sheffield, Sheffield, 2017.

[26] X. Li, G. Shu, H. Tian, L. Shi, G. Huang, T. Chen, and P. Liu, "Preliminary tests on dynamic characteristics of a CO2 transcritical power cycle using an expansion valve in engine waste heat recovery," *Energy,* vol. 140, pp. 696-707, 2017.

[27] F. Alobaid, M. Nicolas, S. Ralf, L. Thomas, H. Christian, and E. Bernd, "Progress in dynamic simulation of thermal power plants," *Progress in Energy and Combustion Science,* vol. 59, pp. 79-162, 2017.

[28] T. A. Horst, H. S. Rottengruber, M. Seifert, and J. Ringler, "Dynamic heat exchanger model for performance prediction and control system design of automotive waste heat recovery systems," *Applied Energy*, vol. 105, pp. 293-303, 2013.

[29] S. Quoilin, R. Aumann, A. Grill, A. Schuster, V. Lemort, and H. Spliethoff, "Dynamic modeling and optimal control strategy of waste heat recovery Organic Rankine Cycles," *Applied Energy*, vol. 88, no. 6, pp. 2183 - 2190, 2011.

[30] G. Shu, X. Wang, H. Tian, P. Liu, D. Jing, and X. Li, "Scan of working fluids based on dynamic response characters for Organic Rankine Cycle using for engine waste heat recovery," *Energy*, vol. 133, pp.609-620, 2017.

[31] M. Jiménez-Arreola, R. Pili, C. Wieland, and A. Romagnoli, "Dynamic study of ORC evaporator operating under fluctuating thermal power from waste heat sources," *Energy Procedia,* vol. 143, pp. 404-409, 2017.

[32] Z. Sun, L. Gao, J. Wang, and Y. Dai, "Dynamic optimal design of a power generation system utilizing industrial waste heat considering parameter fluctuations of exhaust gas," *Energy,* vol. 44, no. 1, pp. 1035-1043, 2012.

[33] A. Hernandez *et al.*, "Design and experimental validation of an adaptive control law to maximize the power generation of a small-scale waste heat recovery system," *Applied Energy,* vol. 203, pp. 549-559, 2017.

[34] X. Li, G. Shu, H. Tian, L. Shi, and X. Wang, "Dynamic Modeling of $CO_2$ Transcritical Power Cycle for Waste Heat Recovery of Gasoline Engines," *Energy Procedia,* vol. 105, pp. 1576-1581, 2017.

[35] J.H. Park, S.W. Bae, H.S. Park, J.E. Cha, and M.H. Kim, "Transient analysis and validation with experimental data of supercritical CO2 integral experiment loop by using MARS," *Energy*, vol. 147, pp.1030-1043, 2018.

[36] J.D. Osorio, R. Hovsapian, and J.C. Ordonez, "Dynamic analysis of concentrated solar supercritical CO2-based power generation closed-loop cycle," *Applied Thermal Engineering*, vol. 93, pp.920-934, 2016.

[37] D. Milani, M.T. Luu, R. McNaughton, and A. Abbas, "A comparative study of solar heliostat assisted supercritical CO2 recompression Brayton cycles: dynamic modelling and control strategies," *The Journal of Supercritical Fluids*, vol. 120, pp.113-124, 2017.

[38] D. Flynn (Ed.), *Thermal Power Plant Simulation and Control (IET Power and Energy Series No. 43)*. London: Institution of Engineering and Technology, 2003.

[39] A. J. Ordys, A. W. Pike, M. A. Johnson, R. M. Katebi, and M. J. Grimble, *Modelling and simulation of power generation plants* (Advances in industrial control). London ; New York: Springer-Verlag, 1994.

[40] M. J. Proctor, W. Yu, R. D. Kirkpatrick, and B. R. Young, "Dynamic modelling and validation of a commercial scale geothermal organic rankine cycle power plant," *Geothermics,* vol. 61, pp. 63-74, 2016/05/01/ 2016.

[41] N. A. Carstens, P. Hejzlar, and M. J. Driscoll, "Control System Strategies and Dynamic Response for Supercritical $CO_2$ Power Conversion Cycles," Center for Advanced Nuclear Energy Systems-MIT Nuclear Engineering Department, Cambridge, MAMIT-GFR-038, 2006, Available: http://nuclear.inl.gov/deliverables/docs/gfr-038.pdf, Accessed on: 05 January 2014.

[42] Y. Gong, N. A. Carstens, M. J. Driscoll, and I. A. Matthews, "Analysis of Radial Compressor Options for Supercritical $CO_2$ Power Conversion Cycles," MIT Center for Advanced Nuclear Energy Systems, Department of Nuclear Science and Engineering, and Gas Turbine Laboratory of the Department of Aeronautics and Astronautics., Cambridge, MAMIT-GFR-034, 2006,

Available: http://nuclear.inl.gov/deliverables/docs/topical_report_mit-gfr-034.pdf, Accessed on: 09 March 2014.

[43] P. Thomas, *Simulation of industrial processes for control engineers*. Oxford: Butterworth-Heinemann, 1999.

[44] O. Olumayegun, M. Wang, and G. Kelsall, "Thermodynamic analysis and preliminary design of closed Brayton cycle using nitrogen as working fluid and coupled to small modular Sodium-cooled fast reactor (SM-SFR)," *Applied Energy,* vol. 191, no. 0, pp. 436-453, 2017.